European Conference on Computational Fluid Dynamics
ECCOMAS CFD 2006
P. Wesseling, E. Oñate and J. Périaux (Eds)

A STABLE PRESSURE-CORRECTION ALGORITHM FOR LOW-SPEED TURBULENT COMBUSTION SIMULATIONS

Pieter Rauwoens*, Krista Nerinckx, Jan Vierendeels, Erik Dick and Bart Merci

Ghent University – UGent, Department of Flow, Heat and Combustion Mechanics
Sint-Pietersnieuwstraat 41, 9000 Gent, Belgium
e-mail: pieter.rauwoens@ugent.be
web page: http://www.floheacom.ugent.be

Key words: Pressure Correction, Low-Mach, Variable Density, Numerical Instability

Abstract. *To perform accurate LES-calculations of low Mach number flows with non-premixed combustion, an efficient, robust and accurate algorithm is needed. So-called pressure-correction methods are efficient algorithms for this purpose. Those methods are well elaborated for flows with constant density. However, in non-premixed combustion simulations, the density is variable in time and space, leading to instabilities. In this paper we provide insight in the origin of the instability by examining the test case of a density jump. Further, we propose improvements to existing schemes in order to increase robustness.*

1 INTRODUCTION

In this research a hybrid RANS-LES turbulence model will be applied in numerical simulations of non-premixed flames with swirl. The finite volume technique is used on a cell-vertex collocated mesh. In order to make an honest judgement of the turbulence model, numerical errors must be sufficiently small. Therefore as a first step, presented here, we develop a sufficiently accurate numerical scheme for low Mach variable density LES-calculations. In this paper efforts are concentrated on the solution algorithm.

The cases considered in this research, as well as many applications in the combustion area, are of low speed nature. This means that the arising velocities are much smaller than the speed of sound, so that density variations due to pressure variations can be neglected. In those so-called low Mach number flows, an efficient way to solve the set of Navier-Stokes equations describing the flow, is to use a segregated solver, relying on a pressure-correction algorithm. Here, the pressure is split in a thermodynamic part p_0 and a second order kinematic pressure p_2, which only appears in the momentum equations. As a result, the momentum equations together with a constraint on the divergence of the velocity decouple from the equations determining the density field. The velocity field

is computed from the momentum equations, and is corrected with a pressure-correction to satisfy the divergence constraint. The correction on the pressure is the result of a Poisson-equation, which is elliptic.

In flows where the density takes a constant value, the classical pressure-correction method of [1] is well elaborated. The velocity at the new time level is predicted from the momentum equations and afterwards corrected in order to obtain a solenoidal field, as imposed by the mass conservation equation. One does not have to fear instabilities arising from the segregated solution procedure when the convective CFL stability condition on the time step is respected.

In order to account for large density variations, in contrast with incompressible constant-density flow calculations, a set of five transport equations needs to be solved in three dimensions: continuity, momentum and a fifth equation, mainly governing the local density. In heat transfer applications this is the energy-equation, whereas in turbulent combustion applications typically the equation for the mixture fraction plays this role. The mixture fraction is a non-dimensional normalized variable which takes the value 0 in pure air and 1 in pure fuel. In non-reacting flows, as is the case in e.g. a turbulent mixing layer, it is the transport equation for the species mass fraction which is density-imposing. Here, we consider from now on the fifth equation as the energy equation.

The pressure-correction formalism in variable density flows consists now of a predictor step for the velocity, obtained from the momentum equations, and a corrector step: the velocity field is corrected to satisfy the continuity equation, or the equation of energy, or a combination of the two. As a result there is not one pressure-correction algorithm, but depending on the choice of the constraining equation, several alternatives are possible.

In this paper, different formulations are investigated. Apparently, some of them fail in giving the correct result when density ratios get too high. The stability of the different schemes is investigated by means of the test case of a density jump. In this test case a jump in density is convected inside a straight 1D channel. It is a simple test case, which yet turns out too difficult to solve with respect to stability for certain widely used pressure-correction algorithms. It is therefore seen as a necessary condition for the eventual scheme to give stable solutions in a general variable-density problem.

Section 2 describes the equations governing the flow field. Section 3 defines the different pressure-correction algorithms. In the fourth section, the density jump as an important test case is explained in more detail. Section 5 shows some results and in the last section the conclusion is stated.

2 GOVERNING EQUATIONS

2.1 Low Mach-Number Formulation

Five equations are considered, governing the conservation of mass, momentum and energy. The Navier-Stokes equations read:

$$\frac{\partial \hat{\rho}}{\partial \hat{t}} + \frac{\partial \hat{\rho}\hat{u}_i}{\partial \hat{x}_i} = 0, \tag{1}$$

$$\frac{\partial \hat{\rho}\hat{u}_j}{\partial \hat{t}} + \frac{\partial \hat{\rho}\hat{u}_i\hat{u}_j}{\partial \hat{x}_i} = -\frac{\partial \hat{p}}{\partial \hat{x}_j} + \frac{\partial \hat{\tau}_{ij}}{\partial \hat{x}_i}, \tag{2}$$

$$\frac{\partial \hat{\rho}\hat{E}}{\partial \hat{t}} + \frac{\partial \hat{\rho}\hat{u}_i\hat{H}}{\partial \hat{x}_i} = \frac{\partial \hat{\tau}_{ij}\hat{u}_j}{\partial \hat{x}_i} + \frac{\partial}{\partial \hat{x}_i}\left(\hat{\kappa}\frac{\partial \hat{T}}{\partial \hat{x}_i}\right), \tag{3}$$

with shear stress tensor $\hat{\tau}$ given by:

$$\hat{\tau}_{ij} = \hat{\mu}\left[\left(\frac{\partial \hat{u}_i}{\partial \hat{x}_j} + \frac{\partial \hat{u}_j}{\partial \hat{x}_i}\right) - \frac{2}{3}\frac{\partial \hat{u}_k}{\partial \hat{x}_k}\delta_{ij}\right]. \tag{4}$$

ρ denotes the local density, u_i the component of the velocity vector in the i-direction, p the pressure, E the total energy per unit of mass, H the total ethalpy per unit of mass, T the temperature and κ the heat conduction coefficient. The $\hat{}$-notation is used to indicate dimensional variables. We assume a perfect and ideal gas, with equation of state:

$$\hat{p} = \hat{\rho}\hat{R}\hat{T}, \tag{5}$$

with R the gas constant. We introduce the nondimensional variables:

$$\begin{gathered}
\rho = \frac{\hat{\rho}}{\hat{\rho}_\infty},\ p = \frac{\hat{p}}{\hat{p}_\infty},\ u_j = \frac{\hat{u_j}}{\hat{u}_\infty}, \\
T = \frac{\hat{T}}{\hat{T}_\infty},\ \mu = \frac{\hat{\mu}}{\hat{\mu}_\infty},\ \kappa = \frac{\hat{\kappa}}{\hat{\kappa}_\infty}, \\
x_j = \frac{\hat{x_j}}{\hat{L}},\ t = \frac{\hat{t}}{\hat{L}/\hat{u}_\infty},\ E = \frac{\hat{E}}{\hat{p}_\infty/\hat{\rho}_\infty},\ H = \frac{\hat{H}}{\hat{p}_\infty/\hat{\rho}_\infty}.
\end{gathered} \tag{6}$$

The subscript ∞ denotes reference values. By doing so, three non-dimensional parameters appear:

$$\tilde{M}_\infty = \frac{\hat{u}_\infty}{\sqrt{\hat{p}_\infty/\hat{\rho}_\infty}},\ Re_\infty = \frac{\hat{\rho}_\infty\hat{u}_\infty\hat{L}}{\hat{\mu}_\infty},\ Pr_\infty = \frac{\hat{c}_p\hat{\mu}_\infty}{\hat{\kappa}_\infty} \tag{7}$$

and the non-dimensional Navier-Stokes equations become

$$\frac{\partial \rho}{\partial t} + \frac{\partial \rho u_i}{\partial x_i} = 0, \tag{8}$$

$$\frac{\partial \rho u_j}{\partial t} + \frac{\partial \rho u_i u_j}{\partial x_i} = -\frac{1}{\tilde{M}_\infty^2}\frac{\partial p}{\partial x_j} + \frac{1}{Re_\infty}\frac{\partial \tau_{ij}}{\partial x_i}, \tag{9}$$

$$\frac{\partial \rho E}{\partial t} + \frac{\partial \rho u_i H}{\partial x_i} = \frac{\tilde{M}_\infty^2}{Re_\infty}\frac{\partial \tau_{ij} u_j}{\partial x_i} + \frac{\gamma}{(\gamma-1)\,Re_\infty Pr_\infty}\frac{\partial}{\partial x_i}\left(\kappa \frac{\partial T}{\partial x_i}\right), \tag{10}$$

with γ the specific heat ratio. The total energy and total enthalpy are given by

$$E = e + \tilde{M}_\infty^2 \frac{1}{2}\left|u\right|^2, \tag{11}$$

$$H = E + \frac{p}{\rho}, \tag{12}$$

with e the internal energy. The nondimensional equations of state become

$$p = \rho T, \tag{13}$$

$$e = \frac{1}{\gamma - 1} T. \tag{14}$$

As we are dealing with low Mach number flows, the set of equations (8)-(10) can be simplified: every variable is expanded in a power series of $\tilde{M}_\infty$, and the asymptotic limit for $\tilde{M}_\infty$ going to zero is taken. For every variable the lowest order term remains in the equations, except for the pressure, which has two parts: a thermodynamic part p_0 and a kinematic part p_2,

$$p = p_0 + \tilde{M}_\infty^2 p_2. \tag{15}$$

The low Mach number equations read [4]:

$$p_0 = p_0(t), \tag{16}$$

$$\frac{\partial \rho}{\partial t} + \frac{\partial \rho u_i}{\partial x_i} = 0, \tag{17}$$

$$\frac{\partial \rho u_j}{\partial t} + \frac{\partial \rho u_i u_j}{\partial x_i} = -\frac{\partial p_2}{\partial x_j} + \frac{1}{Re_\infty}\frac{\partial \tau_{ij}}{\partial x_i}, \tag{18}$$

$$\rho\left[\frac{\partial T}{\partial t} + u_i \frac{\partial T}{\partial x_i}\right] = \frac{1}{Re_\infty Pr_\infty}\frac{\partial}{\partial x_i}\left(\kappa \frac{\partial T}{\partial x_i}\right) + \frac{\gamma - 1}{\gamma}\frac{dp_0}{dt}, \tag{19}$$

and the zeroth-order equation of state is:

$$p_0 = \rho T. \tag{20}$$

Unless we are dealing with enclosed systems, the thermodynamic pressure p_0 has a constant value in time and space.

2.2 Equations for Combustion

The general transport equations, describing a reacting flow, are the conservation equations for species:

$$\frac{\partial \rho Y_l}{\partial t} + \frac{\partial \rho u_i Y_l}{\partial x_i} = \frac{\partial}{\partial x_i}\left(J_{li}\right) + \dot{\omega}_l, \tag{21}$$

with Y_l the mass fraction of species l, J_{li} the diffusive flux and $\dot{\omega}_l$ the chemical source term. If we assume Fick's diffusion law with equal diffusivities for all species and if we neglect the Sorret-effect, these equations can be lumped together into one equation for the mixture fraction ξ:

$$\frac{\partial \rho \xi}{\partial t} + \frac{\partial \rho u_i \xi}{\partial x_i} = \frac{\partial}{\partial x_i}\left(D\frac{\partial \xi}{\partial x_i}\right). \tag{22}$$

As mentioned, the mixture fraction takes a value between 0 and 1 (0 for pure oxidizer and 1 for pure fuel). The advantage of equation (22) is that the chemical source term disappears. Once equation (22) is solved, and the value of ξ is known, the variables Y_l are obtained from the chemistry model. Furthermore in the absence of radiation and under adiabatic circumstances the static enthalpy can immediately be recovered from the mixture fraction. Hence no transport equation for static enthalpy needs to be solved and temperature immediatly follows from the value of ξ. (Note that this is not true when the energy equation is expressed in terms of temperature. In this manner, a source term, expressing the heat generation per unit of time by the exothermal combustion reactions appears.)

3 PRESSURE-CORRECTION ALGORITHMS

In this section we present different formulations of the pressure-correction algorithm. In order to keep the overview, the equations (17) to (19) are simplified to their Euler-formulation by taking the limit $Re_\infty \to \infty$. Furthermore we do not consider enclosures, so p_0 is a constant. Hence the equations to solve become:

$$\frac{\partial \rho}{\partial t} + \frac{\partial \rho u_i}{\partial x_i} = 0, \tag{23}$$

$$\frac{\partial \rho u_j}{\partial t} + \frac{\partial \rho u_i u_j}{\partial x_i} = -\frac{\partial p_2}{\partial x_j}, \tag{24}$$

$$\frac{\partial T}{\partial t} + u_i\frac{\partial T}{\partial x_i} = 0, \tag{25}$$

The prediction of the velocity is the same for all algorithms: the pressure terms in the momentum equations (24) are discretized at the old time level. If we treat the convective terms explicitly, the predicted momentum field $(\rho u_j)^*$ follows from

$$\frac{(\rho u_j)^* - (\rho u_j)^n}{\Delta t} + \left(\frac{\partial \rho u_i u_j}{\partial x_i}\right)^n = -\left(\frac{\partial p_2}{\partial x_j}\right)^n. \tag{26}$$

This field is corrected to give the velocity at the new time level:

$$(\rho u_j)^{n+1} = (\rho u_j)^* + (\rho u_j)', \tag{27}$$

where the correction for the momentum $(\rho u_j)'$ is related to the correction for the pressure $p' = p^{n+1} - p^n$ by

$$\frac{(\rho u_j)'}{\Delta t} = -\frac{\partial p'}{\partial x_j}. \tag{28}$$

Four different formulations of the pressure-correction algorithm are now considered. They differ in two aspects:

1. the determination of the density at the new time level;
2. the constraining equation from which $(\rho u_j)'$ follows.

3.1 Frequently Used Pressure-Correction Algorithms

3.1.1 Standard Pressure-Correction

This version can be considered as a direct extension of the pressure-correction scheme for constant-density flow. The energy-equation (25) is used to calculate the temperature T^{n+1}. The density then follows:

$$\rho^{n+1} = \frac{p_0}{T^{n+1}}. \tag{29}$$

The velocity has to obey the continuity equation (23), written as

$$\left(\frac{\partial \rho u_i}{\partial x_i}\right)^{n+1} = -\frac{\rho^{n+1} - \rho^n}{\Delta t}. \tag{30}$$

Inserting (27) and (28) in (30) results in a Poisson equation for the pressure:

$$\left(\frac{\partial \rho u_i}{\partial x_i}\right)^* - \Delta t \frac{\partial^2 p'}{\partial x_i^2} = -\frac{\rho^{n+1} - \rho^n}{\Delta t}. \tag{31}$$

3.1.2 Constraint-Based Pressure-Correction

For heat transfer applications a constraint, different than the conservation of mass, can be constructed. Indeed, by writing the temperature equation (19) in conservative form, an equation for the thermodynamic pressure is obtained:

$$\frac{dp_0}{dt} + \gamma p_0 \frac{\partial u_i}{\partial x_i} = \frac{\gamma}{Re_\infty Pr_\infty} \frac{\partial}{\partial x_i}\left(\kappa \frac{\partial T}{\partial x_i}\right). \tag{32}$$

When dealing with the Euler-equations in open atmosphere, this simplifies into

$$\frac{\partial u_i}{\partial x_i} = 0, \tag{33}$$

requiring the velocity field to be solenoidal. This gives rise to a Poisson-like pressure equation:

$$\left(\frac{\partial u_i}{\partial x_i}\right)^* - \Delta t \frac{\partial}{\partial x_i}\left(\frac{1}{\rho^{n+1}}\frac{\partial p'}{\partial x_i}\right) = 0, \tag{34}$$

The density field again follows from (25) and (29).

3.2 Improved Pressure-Correction Algorithms

Several arguments form the basis for the improvements, shown in the two following subsections:

- the scheme must remain stable, even in regions with high density jumps;
- mass must be conserved;
- a pressure Poisson-equation with constant coefficients is desirable;
- in statistically steady low-speed non-premixed combustion applications under adiabatic circumstances, no energy-equation is needed at all when unity Lewis Number is assumed for all species since the static enthalpy can then immediately be recovered from the mixture fraction (see section 2.2). Therefore an algorithm which uses a constraint solely based on the energy equation, is not a viable approach.

These arguments result in two improved schemes. A judgement upon which scheme is the best, depends on the specific desire of the user, balancing stability and computing speed.

3.2.1 The Standard Scheme Revised

Using 20 the equation for temperature (25) is rewritten as an equation for density:

$$\frac{\partial \rho}{\partial t} + u_i \frac{\partial \rho}{\partial x_i} = 0, \tag{35}$$

from which the density at the new time level ρ^{n+1} immediately follows. The mass conservation equation (30) is replaced by

$$\left(\frac{\partial \rho u_i}{\partial x_i}\right)^\dagger = -\frac{\rho^{n+1} - \rho^n}{\Delta t}. \tag{36}$$

The dagger-symbol indicates a partly-implicit value given by

$$\begin{aligned}(\rho u)^{\dagger} &= \rho^n u^* + (\rho u)' \\ &= (\rho u)^{n+1} - \left(\rho^{n+1} - \rho^n\right) u^*. \end{aligned} \tag{37}$$

These definitions give rise to a pressure Poisson-equation of the form

$$\frac{\partial \rho^n u_i^*}{\partial x_i} - \Delta t \frac{\partial^2 p'}{\partial x_i^2} = -\frac{\rho^{n+1} - \rho^n}{\Delta t}. \tag{38}$$

The advantage of the latter equation over (31) is that, for a case with pure convective transport of density in a region with constant velocity, (38) gives a constant pressure field, which is physically correct.

3.2.2 The Constraint-Based Correction Revised

The density field at the new time is calculated by using the continuity equation (23), or the equation of temperature in the form (35). The constraint on the velocity field follows from the combination of these two equations. Eliminating the time derivative of the density, we get:

$$\frac{\partial \rho u_i}{\partial x_i} = u_i \frac{\partial \rho}{\partial x_i} \tag{39}$$

If we evaluate the latter equation at time level $n+1$, we can derive the Poisson-like equation

$$\left(\frac{\partial \rho u_i}{\partial x_i}\right)^* - \Delta t \frac{\partial^2 p'}{\partial x_i^2} = \frac{\partial \rho^{n+1}}{\partial x_i} \left[u_i^* - \frac{\Delta t}{\rho^{n+1}} \frac{\partial p'}{\partial x_i}\right]. \tag{40}$$

4 TEST CASE: DENSITY JUMP

Since several authors [3, 5] reported instabilities in non-premixed combustion simulations when the density ratio exceeds a certain value (which is around 4), we take a density jump as test case. In a 1D channel a step in density with height $(\rho_1 - \rho_0)$ is convected with a constant velocity u. No diffusive effects are considered. An inlet boundary condition for the velocity $u = 1$ and density $\rho = 1$ is imposed. At the outlet the pressure is fixed to a value $p_2 = 1$. The thermodynamic pressure p_0 equals an arbitrary strictly positive value. The initial field (Fig. 1) for the density is the piecewise constant function:

$$\rho_i = \begin{cases} 1 & \text{for} \quad i \in [1, i_1[\\ r & \text{for} \quad i \in [i_1, i_2] \\ 1 & \text{for} \quad i \in]i_2, 100] \end{cases}. \tag{41}$$

r is given a value of 20. The interval of the jump is $[20, 40]$. The equations are solved using a finite volume method on a collocated mesh, which means that all variables are

located in the center of the control volume. The pressure term in the momentum equation is discretized centrally. A first order upwinding for the convective terms is used. Also in the conservation equation for mass, the density in the convective term takes the upwind value. Indeed, the continuity equation is seen as a transport equation for density, rather than a conservation (continuity) equation. All calculations are done with a convective CFL-number of 0.9.

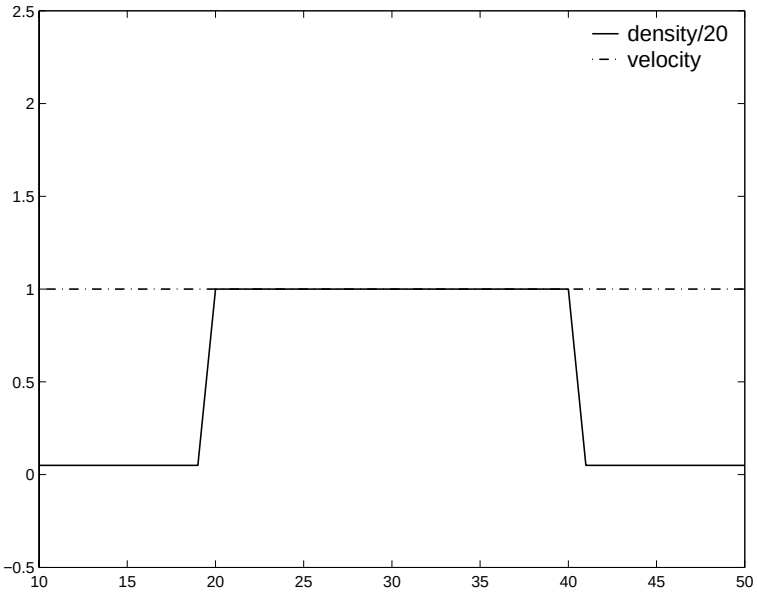

Figure 1: Density jump with factor 20 in a straight channel: initial condition.

5 RESULTS

5.1 Standard Pressure-Correction

Fig. 2 shows that the standard pressure-correction scheme gives inaccurate predictions for the velocity field (dash-dotted line), even in regions far away from the density step ($x > 40$). This observation follows from the corrector step (30) that imposes mass conservation. Since the density field at the new time level follows from the non-conservative discretization (25), mass is conserved through the adjustment of the outlet velocity. From this we see that errors in the calculation of the pressure field have a major influence on the whole domain, and must therefore remain well controlled. One solution for preserving the stability of the scheme is given by an unphysical rescaling of the time derivative of the density [2]. However, since the rescaling factor has to take a value in the order of 1/100, this artificial solution jeopardizes results of time accurate simulations.

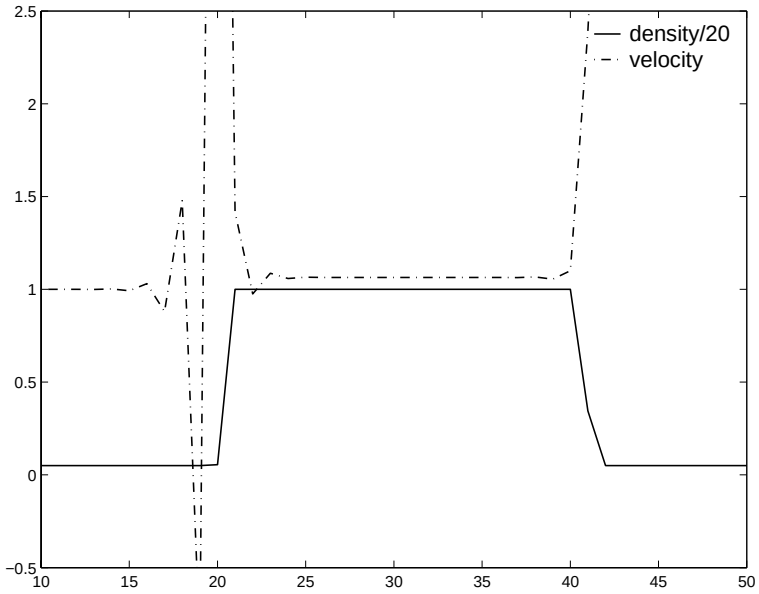

Figure 2: Convection of a density jump with factor 20 in a straight channel after one time step with the Standard Pressure-Correction .

5.2 Constraint-Based Pressure-Correction

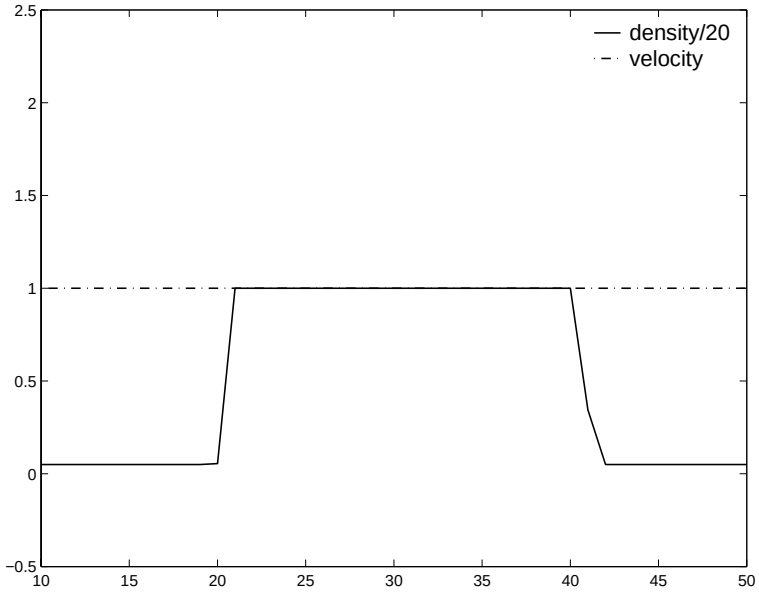

Figure 3: Convection of a density jump with factor 20 in a straight channel after one time step with the Constraint-Based Pressure-Correction Scheme.

This approach gives accurate results: the velocity remains constant during the computation, which is physically correct (Fig. 3). However, when the duct is divergent or convergent, mass is no longer conserved (not shown). Moreover, when this formulation of the pressure-correction algorithm is applied in combustion simulations under the conditions as stated in section 3.2, it cannot be used since equation (32) is not solved any more (the mixture fraction transport equation takes over). For completeness we add that in this formulation, in order to get the pressure field right, one has to add an extra predictor step for the density. However, the inaccurate representation of the pressure has no further consequences for the test case considered here.

5.3 Standard Pressure-Correction in Revised Form

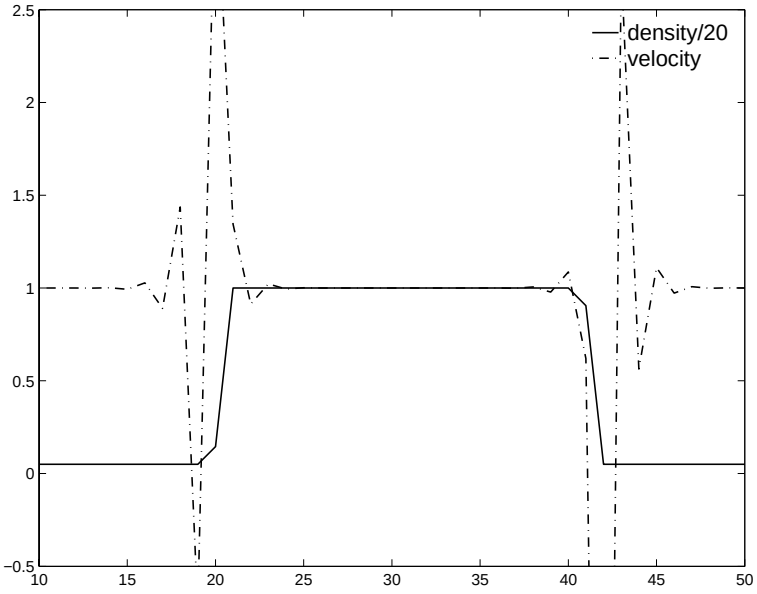

Figure 4: Convection of a density jump with factor 20 in a straight channel after one time step with modified Standard Pressure-Correction.

A way of dealing with the unphysical results from the standard pressure-correction, is by writing (25) in the form (35). The results (Fig. 4) show that wiggles still appear, but the velocity far from the density step is not affected any more.

A second modification (36) makes that the velocity in the straight duct does not alter at all during computation, as is physically correct (Fig. 5). This scheme has the advantage of a low computational cost, because of the constant coefficient Poisson-equation for the pressure (38), but turns out unstable if the density ratio gets too high in a more general environment: e.g. for a divergent channel, the simulation becomes unstable for density ratios higher than a value depending on the section growth. On the other hand, mass is

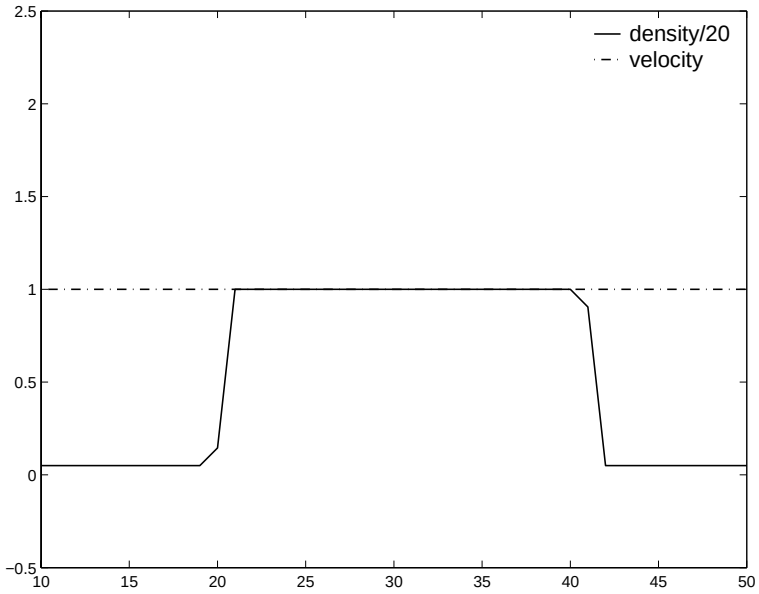

Figure 5: Convection of a density jump with factor 20 in a straight channel after one time step with the Standard Pressure Correction Scheme in revised form.

conserved with this formulation of the scheme.

5.4 Constraint-Based Pressure-Correction in Revised Form

Solutions for the velocity field with the revised form of the constraint-based pressure-correction do not differ from the original formulation for the case of a straight channel (section 5.2), since in either case the velocity remains constant at all times. (The density is again predicted as in section 5.3, so the result is identical to Fig. 5) However, in a more general case, mass is conserved in this approach and the scheme remains stable for high density ratios, even in the divergent channel (up to a density ratio of 10, as required for methane-air combustion simulations). As shown in Fig. 6 for a CFL-number of 0.9 the convection of a density jump in a divergent channel with a section growth of 1% remains stable and the velocity remains practically constant in time, as expected. Because heat transfer is disregarded the smoothing of the density jump is only due to the first order upwind discretization of the scalar field. When performing the same test with a Standard Pressure Correction, results are not physical because even after the first timestep the velocity departs from its orginal value by a factor in the order of 10 (not shown). In contrast with the original constraint correction, this scheme is applicable in the context of non-premixed combustion. The computing time for solving the Poisson-like equation (40) gets higher though, depending on the existing density gradients.

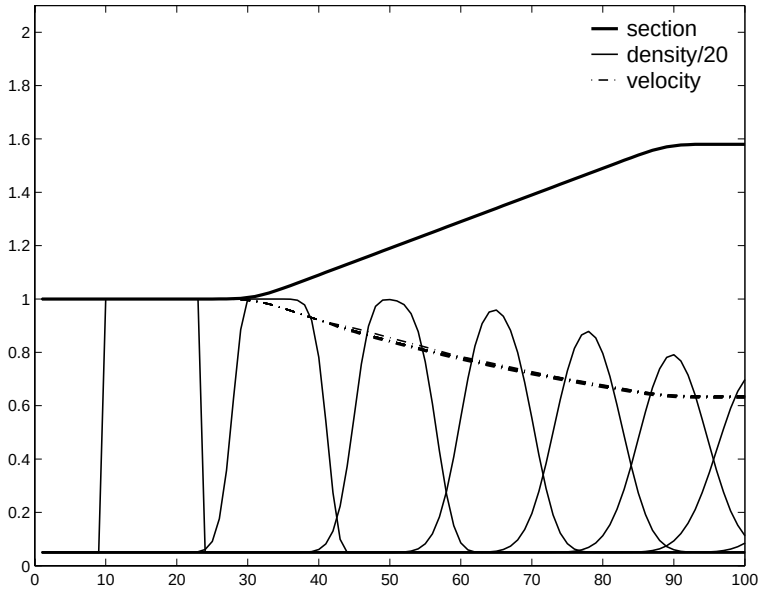

Figure 6: Convection of a density jump with factor 20 in a divergent channel each 20th timestep with the Constraint Pressure-Correction in Revised Form. The velocity remains almost constant.

6 CONCLUSIONS

In this paper we presented four different pressure-correction algorithms for variable-density low-Mach number flow simulations. The standard formulations fail for high density ratios. Two improved schemes were presented: the standard pressure-correction scheme in revised form and the constraint pressure-correction in revised form. The former has a low computational cost for solving the Poisson-equation but has an inherent danger of becoming unstable for too high density ratios, depending on the local flow field. The latter is stable for high density ratios (at least up to a factor of 10) but requires more computing time.

ACKNOWLEDGEMENTS

The second author works as a fellow of the Flemish Institute for the Promotion of Scientific Research in the Industry (IWT).

The fifth author is a Postdoctoral Fellow of the Fund of Scientific Research - Flanders (Belgium) (FWO-Vlaanderen).

REFERENCES

[1] A.J. Chorin, A numerical method for solving incompressible viscous flow problems. *Journal of Computational Physics* **2**, pp.12-26, 1976.

[2] A. Kempf. Large-eddy simulation of non-premixed turbulent flames. *Fortschritt*

Berichte VDI, **6**-513, VDI-Verlag, Düsseldorf, Germany, 2004.

[3] B. Lessani and M.V. Papalexandris. Time-accurate calculation of variable density flows with strong temperature gradients and combustion. *Journal of Computational Physics* **212**, pp.218-246, 2006.

[4] B. Müller. Low Mach number asymptotics of the Navier-Stokes equations. *Journal of Engineering Mathematics*, **34**, pp. 97-109, 1998.

[5] F. Nicoud. Conserative high-order finite-difference schemes for low Mach number flows, *Journal of Computational Physics* **158**, pp.71-97, 2000.